*Int. J. Solids Structures*, 1973, Vol. 9, pp. 217 to 232. Pergamon Press. Printed in Great Britain

# STRESS WAVE PROPAGATION IN A LAMINATED PLATE UNDER IMPULSIVE LOADS

JACOB ABOUDI†

School of Engineering, Tel-Aviv University, Ramat-Aviv, Israel

**Abstract**—The problem of a laminated plate under impulsive normal stress loading is treated. The shearing stress on the surface of the plate is assumed to be zero. The laminates are perpendicular to the plate surfaces. The stresses resulting by the application of the load are computed by a stable finite-difference method which yields reliable results. Illustrations are given for boron–epoxy and glass–epoxy laminates, exhibiting the effect of the reinforcement volume ratios, elastic moduli, observer locations, plate thickness and applied load time durations.

## NOTATION

| | |
|---|---|
| $E$ | Young's modulus |
| $H(t)$ | Heaviside function |
| $2h_1, 2h_2$ | thickness of the layers |
| $l$ | plate thickness |
| $u, v$ | displacement components |
| $t$ | time |
| $x, y$ | cartesian coordinates |
| $\alpha$ | compressional wave velocity |
| $\beta$ | shear wave velocity |
| $\Delta$ | time parameter |
| $\Delta x, \Delta y$ | space increments |
| $\Delta t$ | time step |
| $\lambda, \mu$ | Lamé constants |
| $\nu$ | Poisson ratio |
| $\rho$ | density |
| $\sigma_{ij}$ | stress components |

## INTRODUCTION

THE problem of a laminated composite material excited by an impulsive load is mathematically complicated due to the various boundary and interface conditions involved. In order to avoid the requirement to impose the interface conditions between the fibers and matrix, effective theories can be employed such that the composite can be replaced by a new homogeneous but anisotropic material with average effective elastic constants, see for example the review of Hashin [1]. These theories suffer mainly the disadvantage that they do not predict the dispersion and attenuation caused by the existence of the fibers. In order to take the dispersion into account Voelker and Achenbach [2] treated the problem of a laminated infinite medium composed of two alternating layers which are suddenly subjected to a spatially uniform distribution of transverse forces. The resulting integrals

† Senior Lecturer.

involved were evaluated numerically for small values of time, and were approximated by the method of stationary phase for large values of time.

Peck and Gurtman [3] treated the more complicated problem of an elastic half-space containing two alternating layers. The load on the surface of the half-space is specified by a uniform distribution of normal stresses and vanishing tangential surface displacements. The method of solution is based on the Fourier transform technique and an approximate solution is given by applying the saddle point approximation valid for long times and far field (head of the pulse approximation). In a second paper Whittier and Peck [4] treated this problem experimentally and comparisons were performed between the obtained results and those obtained by the head of the pulse asymptotic approximation.

The more realistic problem in which both normal and tangential stresses are specified on the boundary surface of the half-space is known to be inseparable (in the sense that solutions cannot be obtained by a separation of variables or by a transform technique as was applied in [3]). The three dimensional problem with axial symmetry was treated by Ben-Amotz [5] by employing an asymptotic expansion which is equivalent to the head of the pulse approximation.

Bertholf [6] studied the problem of an axisymmetric elastic wave propagation in a cylindrical rod using a finite difference method. This was extended for variously configured rods by Habberstad [7].

In this paper the problem of a laminated plate composed of two alternating layers is treated. On one surface of the plate a uniform time-dependent normal stress is applied together with zero shear stress. The second surface is assumed to be rigidly clamped. The treatment is based on a finite-difference method which is shown to be stable and yields accurate results. The necessary various numerical treatments of the boundary and interface conditions involved are described.

Illustrations are given for an epoxy matrix with boron and glass layers exhibiting (particularly at the interface between the layers) the effects of reinforcement volume ratios, elastic moduli, observer locations, plate thickness and applied load time durations.

These illustrations display the complete effects of fibers in dynamic loading conditions and provide some information from the point of view of applications.

## STATEMENT OF THE PROBLEM

Consider a plate $0 \leq y \leq l$ consisting of an infinite periodic array of two alternating elastic isotropic layers of width $2h_1$, $2h_2$, respectively with parallel plane boundaries, see Fig. 1(a). At time $t = 0$ a given time-dependent uniform normal stress load starts to act on the plane $y = 0$. The equations of motion with the absence of body forces are:

$$\rho_i \frac{\partial^2}{\partial t^2}\mathbf{u}_i = (\lambda_i + 2\mu_i)\,\text{grad div}\,\mathbf{u}_i - \mu_i\,\text{rot rot}\,\mathbf{u}_i \tag{1}$$

with the initial conditions:

$$\mathbf{u}_i = \frac{\partial}{\partial t}\mathbf{u}_i = 0 \qquad \text{at} \quad t = 0, \qquad i = 1, 2. \tag{2}$$

Here $i = 1, 2$ indexes the two different layers, $\lambda$, $\mu$ are the Lamé constants, $\rho$ is the density and $\mathbf{u}$ is the displacement vector. We consider the problem in which all quantities are

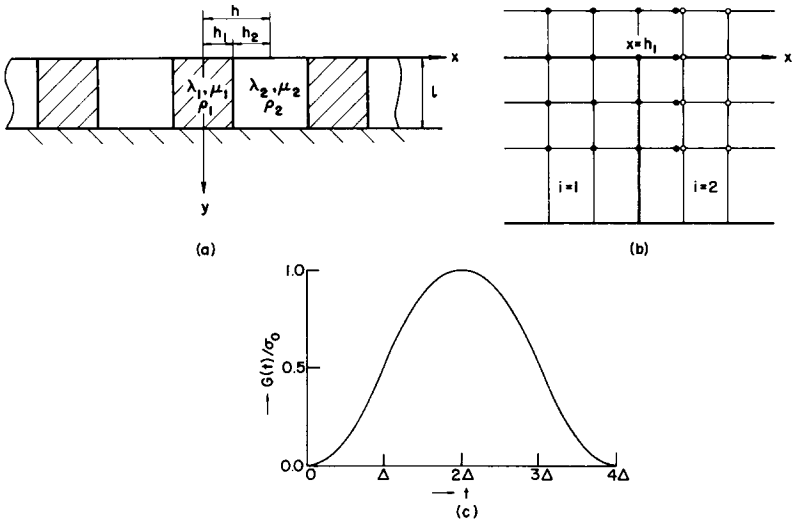


FIG. 1. (a) Geometry of the problem. (b) Grid points near the boundary and interface. (c) Temporal dependence of the applied load.

independent of the Cartesian coordinate $z$ and therefore the displacement components are given by $\mathbf{u}_i = (u_i, v_i, 0)$, $i = 1, 2$. Furthermore due to the uniform extent of the load and the geometry considered, we can restrict ourselves in the region $0 \leq x \leq h$, $0 \leq y \leq l$. The boundary conditions at $y = 0$ are given by:

$$\left.\begin{aligned} \sigma_{xy} &= 0 \\ \sigma_{yy} &= G(t) \end{aligned}\right\} \quad \text{at } y = 0 \tag{3}$$

where $\sigma_{ij}$ are the stress components and $G(t) = 0$ at $t \leq 0$. At $y = l$ rigidly clamped boundary conditions are chosen, i.e.

$$\mathbf{u}(x, l, t) = 0 \quad \text{for all } x \text{ and } t.$$

At the interface $x = h_1$, the normal and tangential displacements and stresses must be continuous:

$$\left.\begin{aligned} u_1 &= u_2 \\ v_1 &= v_2 \\ \sigma_{xy1} &= \sigma_{xy2} \\ \sigma_{xx1} &= \sigma_{xx2} \end{aligned}\right\} \quad \text{at } x = h_1. \tag{4}$$

The symmetry conditions at $x = 0$, $x = h$ are equivalent to the following boundary conditions:

$$\left.\begin{aligned} u &= 0 \\ \sigma_{xy} &= 0 \end{aligned}\right\} \quad \text{at } x = 0, h. \tag{5}$$

The present initial-boundary value problem (1) with (3)–(5) is known to be non-separable, therefore a stable numerical solution will be given here. The accuracy of this solution will be checked and compared with the solution of an elementary case.

## NUMERICAL SOLUTION

Equations (1) can be rewritten in the following matrix form:

$$\frac{\partial^2}{\partial t^2}\mathbf{u}_i = A_i\frac{\partial^2}{\partial x^2}\mathbf{u}_i + B_i\frac{\partial^2}{\partial y^2}\mathbf{u}_i + C_i\frac{\partial^2}{\partial x\partial y}\mathbf{u}_i, \quad i = 1, 2 \tag{6}$$

where

$$A_i = \begin{pmatrix} \alpha_i^2 & 0 \\ 0 & \beta_i^2 \end{pmatrix}, \qquad B_i = \begin{pmatrix} \beta_i^2 & 0 \\ 0 & \alpha_i^2 \end{pmatrix}, \qquad C_i = \begin{pmatrix} 0 & \alpha_i^2 - \beta_i^2 \\ \alpha_i^2 - \beta_i^2 & 0 \end{pmatrix} \tag{7}$$

with

$$\alpha_i = [(\lambda_i + 2\mu_i)/\rho_i]^{\frac{1}{2}}, \qquad \beta_i = [\mu_i/\rho_i]^{\frac{1}{2}}$$

the compressional and shear elastic wave velocities, respectively.

A numerical solution to (6) by a finite difference method is obtained by introducing a grid of mesh sizes $\Delta x$, $\Delta y$, $\Delta t$ and approximating all the derivatives in (6) by a center finite difference expression. Therefore the approximation is correct up to second order in the spatial and temporal increments $\Delta x$, $\Delta y$, $\Delta t$, and the following difference equation is obtained:

$$\begin{aligned} \mathbf{u}_i(x, y, t+\Delta t) = {} & 2[1 - A_i\varepsilon_1^2 - B_i\varepsilon_2^2]\mathbf{u}_i(x, y, t) - \mathbf{u}_i(x, y, t-\Delta t) \\ & + A_i\varepsilon_1^2[\mathbf{u}_i(x+\Delta x, y, t) + \mathbf{u}_i(x-\Delta x, y, t)] \\ & + B_i\varepsilon_2^2[\mathbf{u}_i(x, y+\Delta y, t) + \mathbf{u}_i(x, y-\Delta y, t)] \\ & + C_i\varepsilon_1\varepsilon_2/4[\mathbf{u}_i(x+\Delta x, y+\Delta y, t) + \mathbf{u}_i(x-\Delta x, y-\Delta y, t) \\ & - \mathbf{u}_i(x-\Delta x, y+\Delta y, t) - \mathbf{u}_i(x+\Delta x, y-\Delta y, t)] \\ i = {} & 1, 2 \end{aligned} \tag{8}$$

where

$$\varepsilon_1 = \Delta t/\Delta x, \qquad \varepsilon_2 = \Delta t/\Delta y.$$

According to (8) it is possible to compute the displacements $\mathbf{u}_i$ at time $t+\Delta t$ when the displacement vectors $\mathbf{u}_i$ are known at time $t-\Delta t$ and $t$ for all the interior points of the grid.

A sufficient condition for stability was already obtained for a more general three space dimensional case by Aboudi [8], by using the von Neumann analysis of stability. Such a condition ensures that the difference between the theoretical and numerical solution of the difference equations [in our case equations (8)] remains bounded as the number of the time steps increases. A similar but less involved treatment will lead in the present two spatial dimensional problem to the following condition:

$$(\alpha_i\Delta t/\Delta x)^2 + (\alpha_i\Delta t/\Delta y)^2 \leq 1 \qquad i = 1, 2. \tag{9}$$

Hence the time increment $\Delta t$ must be taken as the minimum obtained from the two conditions given by (9).

The difference scheme (8) is applied to the interior points of the grid. For points which are adjacent to the boundaries at $y = 0$, $x = 0, h$ and the interface at $x = h_1$ special treatments are needed in order to take into account the boundary conditions (3), the interface conditions (4) and the symmetry conditions (5).

(a) *The boundary conditions at* $y = 0$

In order to impose (3), an auxiliary line of grid points at $y = -\Delta y$ is added extending out of the region $y \geq 0$. At each time level $t$ the displacements at the grid points of this line are computed by approximating the derivatives involved in (3) by finite-difference expressions. Although the derivatives with respect to $x$ in (3) are approximated by central differences, it was found that better accuracy is achieved if the derivatives with respect to $y$ are approximated by backward difference expressions. Therefore the displacements on the extra line are given by:

$$\mathbf{u}_i(x, -\Delta y, t) = \mathbf{u}_i(x, 0, t) + D_i[\mathbf{u}_i(x+\Delta x, 0, t) - \mathbf{u}_i(x-\Delta x, 0, t)] - \Delta y F_i \mathbf{G}(t) \qquad i = 1, 2 \quad (10)$$

where

$$D_i = \begin{pmatrix} 0 & \frac{s}{2} \\ \frac{s}{2}\lambda_i/(\lambda_i+2\mu_i) & 0 \end{pmatrix},$$

$$F_i = \begin{pmatrix} 0 & 0 \\ 0 & 1/(\lambda_i+2\mu_i) \end{pmatrix}, \qquad \mathbf{G} = \begin{pmatrix} 0 \\ G(t) \end{pmatrix} \quad (11)$$

and $s = \Delta y/\Delta x$.

According to (10) whenever the values of the displacements at $y = 0$ are known, the displacements at $y = -\Delta y$ are computed, so that they can be used at the next time level to compute the displacements at $y = 0$ by employing (8).

(b) *The interface conditions at* $x = h_1$

Conditions (4) are imposed on the numerical scheme in the following way: the region $i = 1$ (fiber) is extended by adding an auxiliary line at $x = \Delta x$, see Fig. 1(b). Then by taking into account the equality of the displacements at $x = 0$, the last two conditions of the equality of the stresses in (4) are discretized by approximating the derivatives with respect to $y$ by central difference expressions, and the derivatives with respect to $x$ by forward difference expression in region 1 and backward difference expression in region 2. Hence the values of the displacements at the extra line at $x = \Delta x$ are given by:

$$\mathbf{u}^*(\Delta x, y, t) = J\mathbf{u}(0, y, t) + K\mathbf{u}_2(\Delta x, y, t) + L[\mathbf{u}(0, y+\Delta y, t) - \mathbf{u}(0, y-\Delta y, t)], \quad (12)$$

$$\Delta y \leq y \leq l - \Delta y$$

where

$$K = \begin{pmatrix} (\lambda_2+2\mu_2)/(\lambda_1+2\mu_1) & 0 \\ 0 & \mu_2/\mu_1 \end{pmatrix}, \qquad J = I-K,$$

$$L = \begin{pmatrix} 0 & \frac{s}{2}(\lambda_2-\lambda_1)/(\lambda_1+2\mu_1) \\ \mu_2/\mu_1-1 & 0 \end{pmatrix} \tag{13}$$

and $I$ is the unit matrix.

Therefore whenever the values of $\mathbf{u}$ at $x = 0$ and time $t$ are known, the displacements at the auxiliary line can be computed according to (12) in order to use them at the next time level $t+\Delta t$ in (8).

(c) *Computation of the displacements at the two points* $\mathbf{u}(h_1, -\Delta y, t)$, $\mathbf{u}^*(\Delta x, 0, t)$

In order to compute the displacements at the two points $\mathbf{u}(h_1, -\Delta y, t)$, $\mathbf{u}^*(\Delta x, 0, t)$ which belong to the auxiliary lines at $y = -\Delta y$, $x = \Delta x$, respectively, a special treatment must be applied in order to take into account both the boundary conditions (3) and the interface conditions (4) for the stresses at these points. This is achieved by combining equations (10) and (12), forming a system of four algebraic equation with the four unknowns $\mathbf{u}(h_1, -\Delta y, t)$, $\mathbf{u}^*(\Delta x, 0, t)$.

In the special case of equal Lamé constants:

$$\lambda_1 = \lambda_2, \mu_1 = \mu_2, (12) \text{ reduces to } \mathbf{u}^*(\Delta x, y, t) = \mathbf{u}_2(\Delta x, y, t)$$

for all $0 \le y \le l-\Delta y$ as must be. Hence the numerical scheme reduces to that of a homogeneous plate with a loading given by (3).

(d) *Computation of the displacement* $\mathbf{u}^*$ *at the point* $P = (\Delta x, -\Delta y)$

Finally it is required to compute the displacement $\mathbf{u}^*$ at the point $P = (\Delta x, -\Delta y)$, which belongs to the auxiliary line at $x = \Delta x$. This point forms a mathematical singularity due to the requirement to impose both (3) and the last two equations of (4) at $P$. There are several ways to compute the displacement values at $P$. For example we can impose conditions only at $P$ by approximating the derivatives by backward difference expressions. Another possibility is to impose the second condition of (3) and the fourth condition of (4). Both these two possibilities were examined, and it was found that the difference between the two obtained solutions was very small, with a relative error of about 1 per cent, showing that the results are insensitive to both choices we made. This shows that there is no singularity in stress at the edge in the present case. The possibility of the occurrence of such singularity was investigated in the elastostatic problem of two quarter-planes by Bogy [9].

(e) *The symmetry conditions at* $x = 0, h$

At $x = 0, h$ the symmetry conditions (5) must be applied. These conditions imply that:

$$u(0, y, t) = 0, \qquad v(-\Delta x, y, t) = v(\Delta x, y, t) \qquad \text{for } i = 1,$$

and

$$u(h, y, t) = 0, \qquad v(h+\Delta x, y, t) = v(h-\Delta x, y, t) \quad \text{for } i = 2.$$

Therefore the numerical scheme (8) and the boundary conditions (10) must be modified accordingly at $x = 0, h$.

## SPECIFICATION OF THE LOADING FUNCTION AND OTHER PARAMETERS

In order to perform the numerical computations, the loading function $G(t)$ in (3) was chosen as follows:

$$G(t) = \sigma_0\{\delta_2[g(t)] - \delta_2[g(t-2\Delta)]\} \tag{14}$$

$$g(t) = t^2 H(t)/2 \tag{15}$$

Here $H(t)$ is the Heaviside step function, $\sigma_0$ is an amplitude factor which has the dimension of a stress and $\delta_2$ is a second finite difference operator defined by:

$$\delta_2[g(t)] = [g(t) - 2g(t-\Delta) + g(t-2\Delta)]/\Delta^2. \tag{16}$$

The graph of the function $G(t)$ is shown in Fig. 1(c). The parameter $4\Delta$ is the time duration of the applied normal stress on the surface $y = 0$. In the numerical computations we choose for the spatial increments $\Delta x = \Delta y = h/50$. The time increment $\Delta t$ is determined according to (9) as was stated previously. The computations were performed for boron–epoxy and glass–epoxy composites. The material constants are:

TABLE 1

| | $E$ (psi) | $\nu$ | $\rho$ (g/cm$^3$) | $\lambda$ (psi) | $\mu$ (psi) |
|---|---|---|---|---|---|
| Epoxy | $0{\cdot}5 \times 10^6$ | 0·35 | 1·188 | $0{\cdot}43 \times 10^6$ | $0{\cdot}18 \times 10^6$ |
| Boron | $60 \times 10^6$ | 0·2 | 2·63 | $16{\cdot}6 \times 10^6$ | $25 \times 10^6$ |
| Glass | $10{\cdot}5 \times 10^6$ | 0·2 | 2·54 | $2{\cdot}9 \times 10^6$ | $4{\cdot}4 \times 10^6$ |

$E$ is the Young modulus and $\nu$ is the Poisson ratio.

## CHECKING OF THE ACCURACY

In order to check the accuracy of the described finite difference scheme, we compare the results obtained in the special case of equal Lamé constants and densities with the corresponding analytical solution. Indeed in the present case the problem reduces to a one dimensional for which an analytical solution can be obtained by applying Laplace transform. We obtain the following expression for the $y$ component of the displacement (which is independent of $x$):

$$v(y, t) = -k(\tau)/\rho\alpha \tag{17}$$

where:

$$k(\tau) = \sigma_0\{\tau^3 H(\tau) - 2(\tau-\Delta)^3 H(\tau-\Delta) + 2(\tau-3\Delta)^3 H(\tau-3\Delta) - (\tau-4\Delta)^3 H(\tau-4\Delta)\}/6\Delta^2 \tag{18}$$

with

$$\tau = t - y/\alpha, \qquad \alpha^2 = (\lambda+2\mu)/\rho. \tag{19}$$

The stress $\sigma_{yy}$ is given by

$$\sigma_{yy}(y, t) = \frac{\partial k(\tau)}{\partial \tau}. \tag{20}$$

The present solution (17)–(20) of the one dimensional problem is valid for $0 \leq t \leq l/\alpha$, since it does not take into account waves which are reflected back from $y = l$. The complete solution which contains all the reflection can be obtained similarly.

In Fig. 2(a) the displacement $v$ and the stress $\sigma_{yy}$ are shown at $y = l/5$ as a function of the non-dimensional time $\alpha t/l$, for the pulse time duration $4\alpha\Delta/l = 0{\cdot}3$.

The present analytical solution of the one dimensional problem serves as a check on the accuracy of the results of the previous finite difference scheme in two space dimensions and time as is determined in equations (8)–(13). In Table 2 a comparison between the two solutions for the displacement at $y = l/5$ is shown at the time interval $0{\cdot}35 \leq \alpha t/l \leq 0{\cdot}5$ which is within the rise time of the displacement to its maximum value at $\alpha t/l = 0{\cdot}5$. It is seen that excellent correspondence between the two solutions is obtained. The maximum relative error is about 0·5 per cent. The horizontal displacement obtained by the numerical solution is of order of $10^{-14}$.

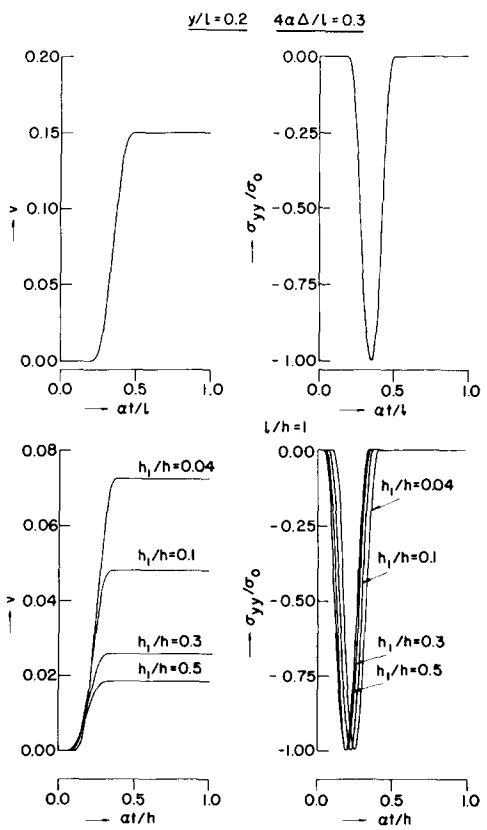


FIG. 2. Vertical displacement and normal stress obtained at $y/l = 0{\cdot}2$ in the one-dimensional problem (top). Vertical displacements and normal stresses obtained at $y/l = 0{\cdot}2$ according to the effective modulus theory (bottom).

TABLE 2

| $\alpha t/l$ | $v/l$ Analytical solution | $v/l$ Numerical solution | $\sigma_{yy}/\sigma_0$ Analytical solution | $\sigma_{yy}/\sigma_0$ Numerical solution |
|---|---|---|---|---|
| 0·35 | 0·0750 | 0·0745 | −1·0000 | −0·9941 |
| 0·36 | 0·0850 | 0·0845 | −0·9911 | −0·9815 |
| 0·37 | 0·0976 | 0·0942 | −0·9644 | −0·9527 |
| 0·38 | 0·1042 | 0·1037 | −0·9200 | −0·9084 |
| 0·39 | 0·1131 | 0·1125 | −0·8577 | −0·8488 |
| 0·40 | 0·1213 | 0·1208 | −0·7777 | −0·7734 |
| 0·41 | 0·1286 | 0·1281 | −0·6800 | −0·6825 |
| 0·42 | 0·1348 | 0·1345 | −0·5644 | −0·5786 |
| 0·43 | 0·1398 | 0·1398 | −0·4355 | −0·4666 |
| 0·44 | 0·1436 | 0·1439 | −0·3200 | −0·3537 |
| 0·45 | 0·1463 | 0·1468 | −0·2222 | −0·2478 |
| 0·46 | 0·1481 | 0·1487 | −0·1422 | −0·1565 |
| 0·47 | 0·1492 | 0·1498 | −0·0800 | −0·0846 |
| 0·48 | 0·1497 | 0·1502 | −0·0355 | −0·0343 |
| 0·49 | 0·1499 | 0·1500 | −0·0088 | −0·0041 |
| ≥0·50 | 0·1500 | 0·1499 | 0 | |

Similarly, the analytical and numerical solutions for the stresses are shown at this interval. Here again the agreement between the two solutions is well seen.

In addition to the above checks, we also performed a comparison between the results obtained with different choices of mesh sizes. We found that for the pulse width $4\alpha\Delta/h = 0{\cdot}3$ and mesh sizes $\Delta x = \Delta y = h/50$, the obtained results (in the two space dimension problem) are reliable and the network system yields sufficient accuracy.

## EFFECTIVE MODULUS THEORY

It is interesting to show some results based upon the effective modulus theory. According to this theory the composite is replaced by a homogeneous but transversely isotropic medium whose elastic moduli and average density are expressed in terms of the thickness and the material constants of the layers. The expressions of the effective constants can be derived on basis of static [10] or dynamic [11] considerations. In the present case (17)–(20) can be applied with:

$$\rho = (\rho_1 h_1 + \rho_2 h_2)/h \tag{21}$$

$$\alpha = \sqrt{(c_{11}/\rho)} \tag{22}$$

with $c_{11}$ given by:

$$c_{11} = [h^2(\lambda_1 + 2\mu_1)(\lambda_2 + 2\mu_2) + 4h_1 h_2(\mu_1 - \mu_2)(\lambda_1 + \mu_1 - \lambda_2 - \mu_2)]/h'$$

$$h' = h[h_1(\lambda_2 + 2\mu_2) + h_2(\lambda_1 + 2\mu_1)]. \tag{23}$$

In this one dimensional problem the shear stress $\sigma_{xy} = 0$. In Fig. 2(b) the displacement $v$ and normal stress $\sigma_{yy}$ is shown for boron–epoxy at $y = 0{\cdot}2l$ with $h_1/h = 0{\cdot}04$, 0·1, 0·3, 0·5. These curves are shown for the sake of comparison with the corresponding results obtained in the following.

## RESULTS

In the following we examine the results obtained for various reinforcements $h_1/h$, elastic moduli, observer locations, plate thickness and applied pulse time duration.

(a) *Effect of reinforcement changes*

In order to show the effect of various reinforcement on the obtained stresses, we show in Fig. 3 the stresses $\sigma_{xx}$, $\sigma_{xy}$ and $\sigma_{yy}$ at the interface $x = h_1$ and $y = h/10$, where $h_1$ attains the following values: $h_1/h = 0{\cdot}04$, $0{\cdot}1$, $0{\cdot}2$, $0{\cdot}3$, $0{\cdot}4$, $0{\cdot}5$.

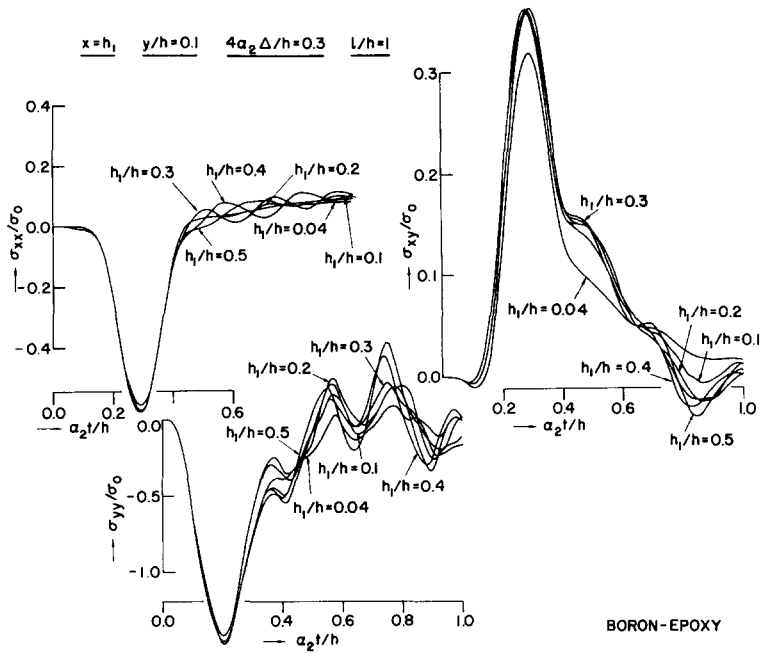


FIG. 3. Time variation of the interface stresses for different reinforcement volumes.

It is seen that minor changes take place with respect to the temporal behavior of $\sigma_{xx}$. The oscillations which appear after the main disturbance as a result of the dispersion are well seen for the higher volume fractions $h_1/h = 0{\cdot}4$, $0{\cdot}5$. These are similarly seen in the plots of the normal stresses $\sigma_{yy}$ and the interface stresses $\sigma_{xy}$. Note that the shear stress at the interface in case of the smallest reinforcement $h_1/h = 0{\cdot}04$ has the lower amplitude as compared with the other values of reinforcement.

Another comparison between the various reinforcement is obtained by displaying the stresses along the interfaces $x = h_1$ at a given time. This is shown in Fig. 4 at $\alpha_2 t/h = 0{\cdot}4$. Here again the stresses $\sigma_{xx}$ have fairly the same behavior. A careful examination of the numerical values of the interface shear stress $\sigma_{xy}$ shows that the smallest volume fraction $h_1/h = 0{\cdot}04$ yields the lowest value as well. When $h_1/h$ increases the amplitude of $\sigma_{xy}$ increases and it attains its maximum when $h_1/h = 0{\cdot}3$ after which it decreases again. This behavior is with accordance of the results of Ben-Amotz [5]. Figure 4 shows also that the

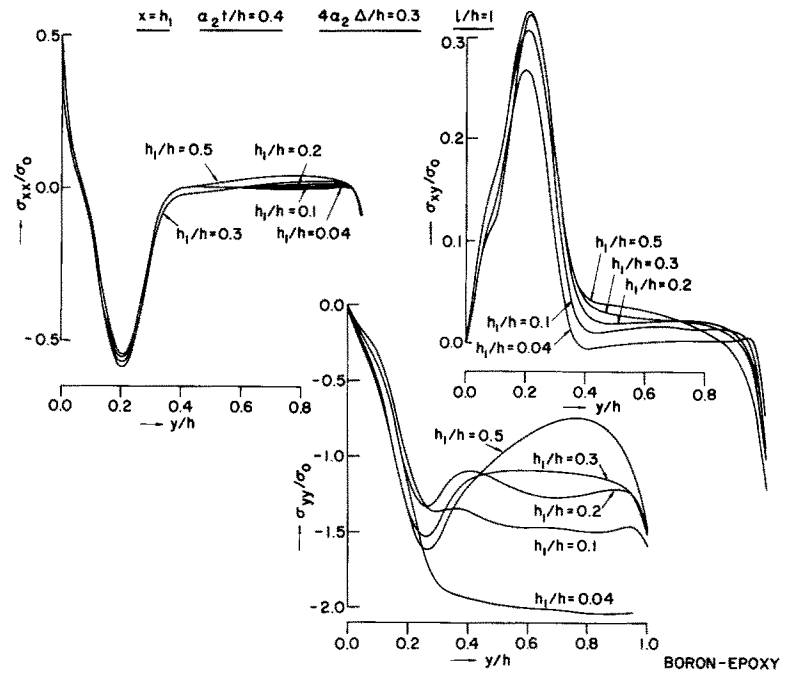


FIG. 4. Variation of stresses along the interface for different reinforcement volumes.

normal stress $\sigma_{yy}$ attains its maximum for the lowest reinforcement $h_1/h = 0{\cdot}04$. In this case $\sigma_{yy}$ is twice larger than the normal stress input $\sigma_0$ on the surface, or the normal stress predicted by the effective modulus theory. Therefore a quite large magnification of the normal stress occurs. It may be noted that according to both Figs. 3 and 4, $\sigma_{yy}$ is more than two order of magnitude larger than $\sigma_{xx}$ and $\sigma_{xy}$.

(b) *Effect of elastic moduli*

In order to examine the effect of elastic moduli variations we compare two kinds of reinforcements: boron–epoxy and glass–epoxy. In Fig. 5 the dependence of the stresses on both the time $t$ and the distance $y$ along the interface is shown for these two composites. The oscillations as a result of the dispersion in the case of the boron–epoxy reinforcement are more pronounced. This is with accordance of the results of Peck and Gurtman [3] that the dispersion is higher for the larger contrast in modulus between the fiber and matrix.

The shear stress $\sigma_{xy}$ at the interface is larger in the boron–epoxy as is well seen in the figure, which is again in accordance with the results in [5]. Similar conclusion is valid for the other stresses $\sigma_{xx}$, $\sigma_{yy}$.

In Fig. 6 another comparison between boron–epoxy and glass–epoxy reinforcements is shown with the previous volume fraction $h_1/h = 0{\cdot}3$, but with observation points located at $x/h = 0{\cdot}1$ and $x/h = 0{\cdot}5$. These two values correspond to observation points within the fiber and matrix regions, respectively. As can be expected when the location is within the fiber region, the dispersion is highly pronounced especially in the higher moduli fibers. On

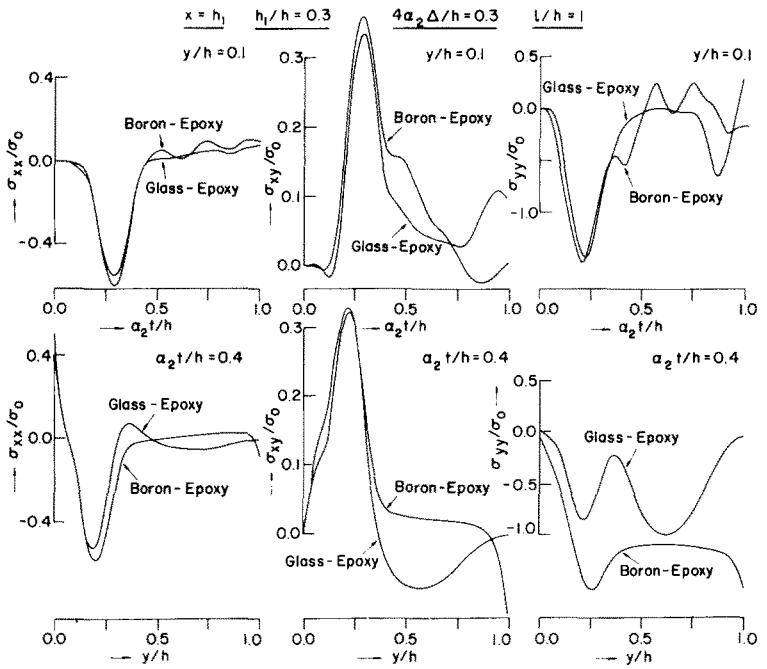


FIG. 5. Dependence of the interface stresses on time and distance along the interface for boron–epoxy and glass–epoxy laminates.

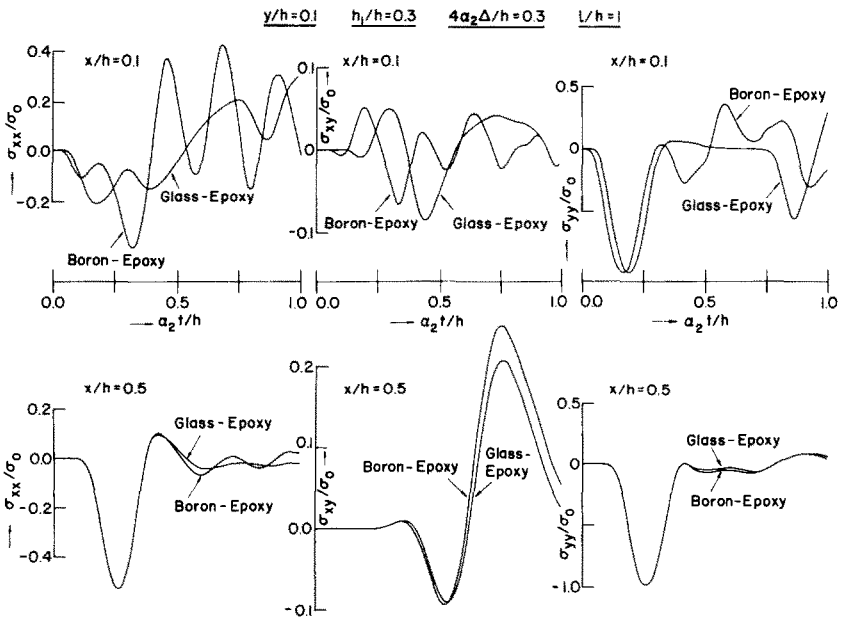


FIG. 6. Time variation of the stresses at two observation points $x/h = 0.1, 0.5$ for boron–epoxy and glass–epoxy laminates.

the other hand there are only small differences between the behavior of the stresses when the location is within the matrix region. These differences become smaller for larger values of $x/h$ where the effect of different fibers is very weak.

(c) *Effect of observer locations*

Let us examine now the behavior of the stresses recorded at various observation points in a given system of a laminated plate. In Fig. 7 the stresses at various distances $x/h$ are shown in the case of a boron–epoxy composite with $h_1/h = 0{\cdot}5$. The upper and lower

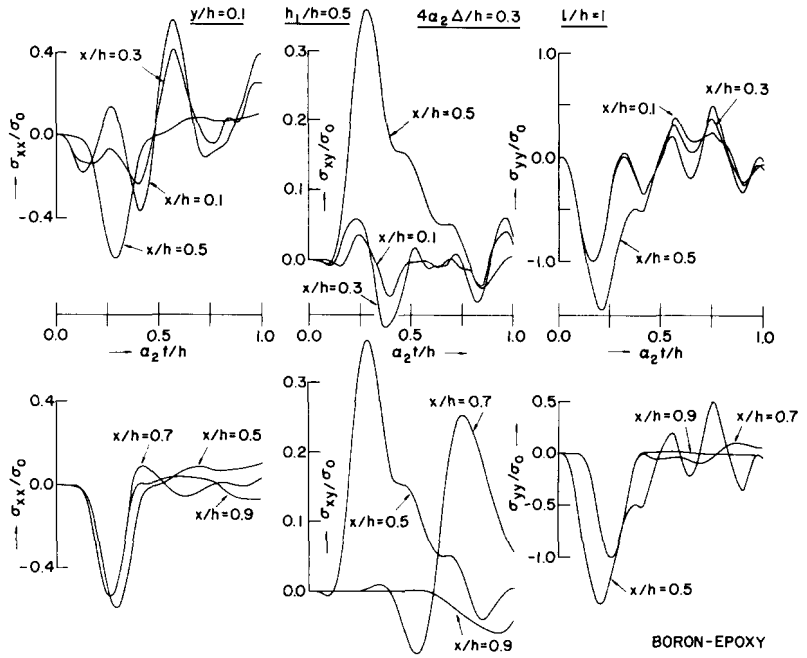


FIG. 7. Variation of stresses at different locations within layer 1 (top) and layer 2 (bottom).

plots in the figure show the stress waves within the fiber and matrix, respectively. The dispersion of the stress wave $\sigma_{xx}$ is higher for the lower values of $x/h$ within the fiber and higher amplitudes are obtained there. On the other hand the shear stress $\sigma_{xy}$ starts from zero at $x = 0$ and it attains its largest value at the interface $x = h_1$. It is more than two times larger than the shear stress obtained at other points in the fiber (with the same value of $y$). The normal stress $\sigma_{yy}$ similarly to $\sigma_{xy}$ attains its maximum value at the interface, but this is much less pronounced as in the case of $\sigma_{xy}$.

Within the matrix $\sigma_{xx}$ has approximately the same amplitude at the various values of $x/h$. On the other hand amplitude of $\sigma_{xy}$ decreases again as the distance from the interface increases, and it vanishes at $x = h$. At various locations $x/h$, the amplitude of the normal stress $\sigma_{yy}$ is reserved except on the interface where it attains its maximum.

In Fig. 8 the temporal variation of the stresses at the interface between the boron and epoxy is shown for several depth locations: $y/h = 0{\cdot}1, 0{\cdot}2, 0{\cdot}3$. It is seen that apart from the

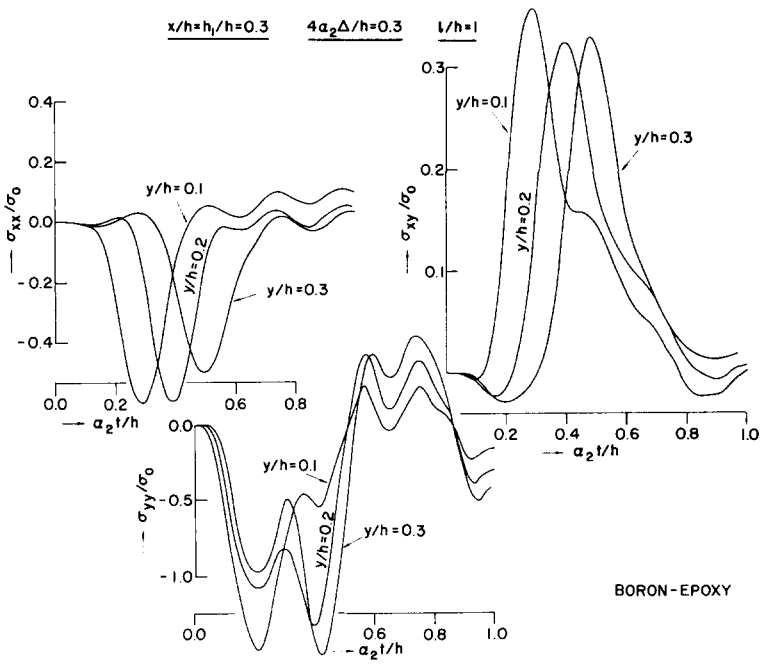


FIG. 8. Time variation of the interface stresses at different observer depth locations.

difference between the arrival times of the main disturbance to the different observation points, the general features of the waves are similar.

(d) *Effect of plate thickness*

In Fig. 9 the stresses at the interface are shown for two choices of the plate thickness: $l/h = 0{\cdot}5, 1$ with $h_1/h = 0{\cdot}3$. It is clearly seen that while the effect on the stress $\sigma_{xx}$ is small,

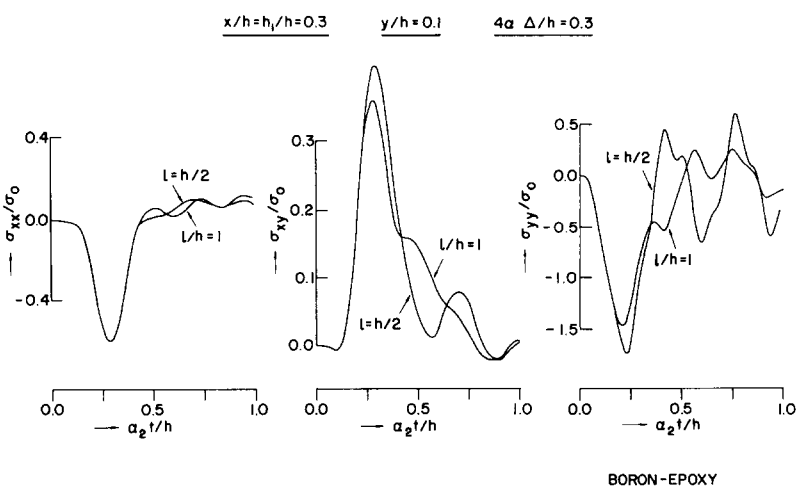


FIG. 9. Time variation of the interface stresses for the two plate thickness $l/h = 0{\cdot}5, 1$.

the shear and normal stresses are sensitive to variations in plate thickness. Both these two stresses have larger amplitudes in the thinner plate. In other words the normal and shear interface stresses increase when the ratio of the fiber spacing distance to the composite thickness increases, see also [5]. We note that the figure shows clearly the effect of the reflections from the boundary at $y = l$.

(e) *Effect of pulse time duration*

All computations reported previously we performed with the time pulse duration $4\Delta = 0{\cdot}3h/\alpha_2$. In Fig. 10 we display the temporal form at the interface and variation with distance along the interface of the stresses for two time loading: $4\alpha_2/h = 0{\cdot}15, 0{\cdot}3$. For the shorter time-duration the dispersion is more pronounced due to the high frequency components content of the pulse, and the amplitudes are smaller. This feature, especially the amplitude damping shows that the stresses are sensitive to the pulse time duration.

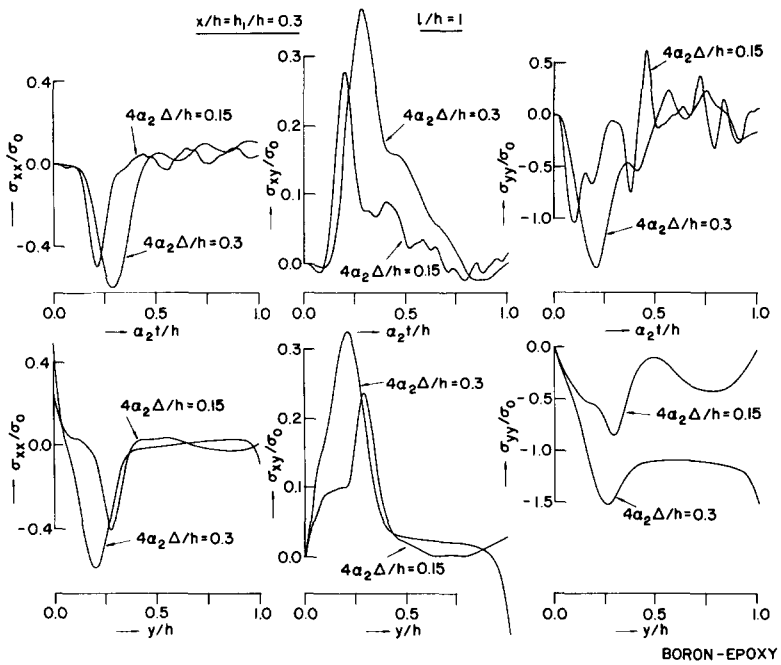


FIG. 10. Dependence of the interface stresses on time and distance along the interface for the two pulse time durations: $4\alpha_2\Delta/h = 0{\cdot}15, 0{\cdot}3$.

*Acknowledgments*—This work was performed under contract AFOSR-71-2143 of the U.S. Air Force. The author wishes to express his sincere thanks for this financial support. The computations reported in this paper were carried out on the CDC-6600 computer at the Tel-Aviv University Computation Center.

## REFERENCES

[1] Z. HASHIN, Theory of Composite Materials, Mechanics of Composite Materials, *Proc. of the 5th Symposium on Naval Structure Mechanics*. Pergamon Press (1970).

[2] L. E. VOELKER and J. D. ACHENBACH, Stress waves in a laminated medium generated by transverse forces. *J. acoust. Soc. Am.* **46**, 1213–1222 (1969).

[3] J. C. PECK and G. A. GURTMAN, Dispersive pulse propagation parallel to the interfaces of a laminated composite. *J. appl. Mech.* **36**, 479–484 (1969).

[4] J. S. WHITTIER and J. C. PECK, Experiments on dispersive pulse propagation in laminated composites and comparison with theory. *J. appl. Mech.* **36**, 485–490 (1969).
[5] M. BEN-AMOTZ, Stress Wave Propagation in Unidirectionally Reinforced Composites, *Recent Advances in Engineering Sciences*, edited by C. ERINGEN, Vol. 5. Gordon and Breach (1970).
[6] L. D. BERTHOLF, Numerical solution for two-dimensional elastic wave propagation in finite bars. *J. appl. Mech.* **34**, 725–734 (1967).
[7] J. L. HABBERSTAD, A two-dimensional numerical solution for elastic waves in variously configured rods. *J. appl. Mech.* **38**, 62–70 (1971).
[8] J. ABOUDI, Numerical simulation of seismic sources. *Geophysics* **36**, 810–821 (1971).
[9] D. B. BOGY, On the problem of edge-bonded elastic quarter-planes loaded at the boundary. *Int. J. Solids Struct.* **6**, 1287–1313 (1970).
[10] G. W. POSTMA, Wave propagation in a stratified medium. *Geophysics* **20**, 780–806 (1955).
[11] S. M. RYTOV, Acoustical properties of a thinly laminated medium. *Soviet Phys. Acoust.* **2**, 68–80 (1956).

(*Received* 15 *December* 1971; *revised* 3 *May* 1972)

**Абстракт**—Обсуждается задача слоистой пластинки под влиянием импульсивной нагрузки нормального напряжения. Предполагается нулевое напряжение сдвига на поверхности пластинки. Слой перпендикулярный к поверхностям пластинки. Вычисляются напряжения, происходящие в результате применения нагрузки, с помощью стабильного метода в конечных разностях, который дает надёжные результаты. Даются иллюстрации для слоев, изтовленных из бороэпоксида и стеклоэпоксида, которые указывают эффект процента армирования, упругих модулей, расположения наблюдения, толщины пластинки и длительность приложенной во времени нагрузки.